JOURNAL OF PROPULSION AND POWER
Vol. 26, No. 6, November–December 2010

# Torsion Pendulum Investigation of Electromagnetic Inertia Manipulation Thrusting

Ricardo L. Marini* and Eugenio S. Galian†
*Instituto Universitario Aeronáutico, X5010JMN Córdoba, Argentina*

DOI: 10.2514/1.46541

**New experimental results on propellantless propulsion by means of electromagnetic inertia manipulation are shown and discussed here and compared with previous results obtained with a flexion pendulum setup, which would have shown the existence of an oscillating force, taken as a genuine propulsive effect. The new results conclusively show that the devices tested do not produce the thrusts predicted by the theory, or those supposedly obtained before with the flexion pendulum, not even up to almost 2 orders of magnitude lower. This strongly suggests that the positive results obtained with the flexion pendulum would have been produced by spurious effects, very likely forces caused by electromagnetic interaction among some components of the electric circuit, which were not appropriately estimated.**

## Nomenclature

| | | |
|---|---|---|
| $A_c$ | = | calculated linear amplitude of oscillation, mm |
| $A_m$ | = | measured amplitude of oscillation, mm |
| $d$ | = | distance from recording plate to torsion pendulum, m |
| $\mathrm{d}t$ | = | time step, s |
| $d_w$ | = | suspending-wire diameter, m |
| $F$ | = | force thrust, N |
| $f$ | = | frequency, Hz |
| $G$ | = | shear modulus, GPa |
| $g$ | = | acceleration of gravity, $\mathrm{m/s^2}$ |
| $I$ | = | moment of inertia, $\mathrm{kg\,m^2}$ |
| $k$ | = | suspending-wire torsion stiffness, Nm/rad |
| $l_t$ | = | thread length, m |
| $l_w$ | = | suspending-wire length, m |
| $M$ | = | moment, Nm |
| $m$ | = | mass of little pendulum, kg |
| $m_e$ | = | equivalent mass, kg |
| $m_t$ | = | mass of thread, kg |
| $n$ | = | number of oscillations |
| $p$ | = | damping factor |
| $r$ | = | distance from action line of thrust to suspending wire, m |
| Sd | = | standard deviation, mm |
| $T$ | = | period of pendulum, s |
| $x$ | = | general linear position, mm |
| $x_c$ | = | calculated linear position, mm |
| $x_m$ | = | measured linear position, mm |
| $\Delta$ | = | angular amplitude of oscillation, rad |
| $\Delta\theta$ | = | angular displacement, rad |
| $\Delta_0$ | = | angular amplitude of oscillation without damping, rad |
| $\delta$ | = | linear displacement, mm |
| $\theta$ | = | angular position, rad |
| $\sigma$ | = | mean quadratic error, mm |

## I. Introduction

EITHER for long space travels or merely to cut down space transportation costs, it is necessary to find new propulsion mechanisms that do not require the enormous amount of propellant used as reaction mass. Several theoretical works show that propulsion could be achieved by manipulating the spaceship inertia in this way: by considering space–time instead of three-space, the spaceship four velocity can be changed by manipulating its mass tensor components. To do that, the fields the spaceship eventually generates must be considered, and so a thrust appears on the material spaceship by means of momentum exchange with its field counterpart. In [1], the theoretical fundamentals of a propulsion system based on electromagnetic inertia manipulation were presented, along with some experimental results from tests carried out with a flexion pendulum, mounting the device as a seismic mass atop a thin vertical cantilever beam (a resonant blade), sitting on a vibration-free platform. Piezoceramic strain transducers were used to detect the seismic mass displacements. The setup was periodically excited by the device with a frequency close to some of its natural ones, in order to magnify the displacements. The thrust would come from the particular electric and magnetic fields distribution, namely, crossed fields produced by an annular capacitor and a toroidal coil appropriately arranged and harmonically excited with an adequate phase shift of current and voltage. The momentum of the electromagnetic field is then balanced by an equal but opposite momentum of the material frame in order to keep constant the total momentum. Thus, a propulsive force appears as a consequence. A further revision [2] suggested that no propulsive force could be produced in the way proposed in [1]. In fact, there is neither transfer of matter nor energy with the rest of the universe; thus, the device operates as a closed system. The momentum of the electromagnetic field comes from the work made by the power supply to introduce the electric charges in the capacitor and to circulate the electrical current in the coil against the induced counterelectromotive force. That is, the momentum is associated with an energy transfer. Therefore, an impulse equal to the electromagnetic momentum but, in the opposite sense, acts on the power supply, and an impulse equal to the momentum appears in the capacitor–coil system while the energy is stored in them. If the electromagnetic field remains attached to the material frame (capacitor and coil) (that is, if the energy transferred from the power supply is not expelled out of the system in a directional beam), the total resultant impulse is null, and no net force is produced. This case would be similar to that of a rocket motor, where the momentum of the exhaust comes from the impulse produced by forces that, acting on the frame in the opposite sense, produce the thrust. But if the device works as a closed system, catching its own exhaust, the momentum is recovered and an impulse equal to the momentum acts on the frame; therefore, no net thrust is produced.

Besides this, since neither the capacitors nor the coils dissipate energy (at least as ideal devices), the work produced by the thrust would be done without spend energy, and so the propulsion system would be a perpetual motion machine.

Received 29 July 2009; revision received 14 June 2010; accepted for publication 19 August 2010. 

*Aeronautical Engineer, Centro de Investigaciones Aplicadas, Avenida Fuerza Aérea 6500.

†Mechanical Engineer, Centro de Investigaciones Aplicadas, Avenida Fuerza Aérea 6500.

On the other hand, the methodology and setup used in those tests would not be appropriated for detecting and measuring a net propulsive force, since the same output signal could also be produced by a mere oscillating force with a null resultant. Therefore, with this setup, the existence of a real propulsive force cannot be conclusively demonstrated; hence, the purpose of the experiment is not fulfilled.

The objective of the present work is to investigate the hypothetical propulsive effect using a torsion pendulum as the method of force measurement, since it can detect and measure a net force but is insensitive to oscillating forces of much higher frequencies than its natural one, so unambiguous and conclusive results could be obtained. It must be remarked that this work was carried out as an independent investigation about the existence of a propulsive force for practical purposes and not for elucidating any other purely theoretical question.

## II. Experimental Setup and Configuration

### A. Torsion Pendulum Design

The pendulum consisted of a horizontal arm suspended about the middle by a steel fiber. The arm supported the thruster (including the power supply) at one end and a balancing weight on the other. To avoid environmental disturbances, the pendulum was enclosed in an acrylic box, passing the suspension wire through a small hole in the cap of the box. The air contained in the chamber contributed to the damping of the pendulum. At the bottom of the motor case, a small blade was attached. The blade was partially submerged in oil, contained in a tray placed under the pendulum, acting as a damper. Deflections of the torsion arm were detected by the motion of a laser beam, reflected on a mirror placed at the suspending point of the torsion arm. The laser beam was directed onto a flat plate outside the acrylic chamber, placed nearly 5 m from it, where the endpoints of oscillations were registered by eye on a sheet of paper. The position of each endpoint was measured from the intersection line of the registering plate, with the plane perpendicular to it passing by the suspending wire of the pendulum.

To estimate the sensitivity of the pendulum, a preliminary design for simulations was considered. The moment of inertia of this pendulum was 0.6 $\mathrm{Kg\,m^2}$ (the estimated value for the actual pendulum according to the mass and dimensions of the device to be tested and the balancing weight). The minimum size of steel wire that could reasonably hold the arm and tensioning mass was found to be of 0.65 mm. A 0.8-mm-diam wire was chosen for safety, in foresight of a further increase of the actual suspending weight. The maximum length of the wire would be about 2.4 m. The torsion stiffness was estimated by means of

$$k = \frac{\pi\, d_w^4}{32\, l_w}\, G \tag{1}$$

The shear modulus $G$ for steel is 79 GPa. With the diameter and length specified previously, a value of about $1.3 \times 10^{-3}$ Nm/rad resulted for the torsion stiffness. The motion of the pendulum was predicted by means of the differential equation,

$$\frac{\mathrm{d}^2\theta}{\mathrm{d}t^2} + 2p\frac{\mathrm{d}\theta}{\mathrm{d}t} + \frac{k}{I}\theta = \frac{F\, r}{I} \tag{2}$$

where the damping factor $p$ was not taken into account for the preliminary estimations because it was still unknown. Equation (2) was solved both analytically and numerically to assure the accuracy of the results. The numerical and analytical results were coincident up to the sixth significant digit. As the expected theoretical thrust was about 300 $\mu$N, to estimate the sensibility of the pendulum, the calculations were carried out for thrusts of 300, 30, and 3 $\mu$N, acting by 20 s (the maximum admissible action time of the thruster) at a distance of 220 mm from the suspending wire, with an initial oscillation angle of 0.01 radians. These values were an estimation of those that would correspond to the actual pendulum. The maximum calculated increments of the angular amplitudes of oscillation of the pendulum $\Delta\theta$ and linear displacement $\delta$ of the laser dot on the plate, with respect to no acting force, are shown on Table 1.

**Table 1 Expected amplitude increments**

| $F$, $\mu$N | $\Delta\theta$, rad | $\delta$, mm |
|---|---|---|
| 300 | 0.038 | 380 |
| 30 | 0.0038 | 38 |
| 3 | 0.00038 | 3.8 |

Therefore, although the accuracy of the results would be affected by the experimental errors, it is certain that a force of about 5 $\mu$N could be detected with this pendulum without using complex optical sensors.

### B. Experimental Procedure

The diameter of the laser dot on the plate was about 12 mm. To improve the accuracy of the measures, the laser beam did not fall directly on the plate but on a little piece of paper, which was manually positioned near the expected endpoint of each oscillation, following the motion of the laser dot until it stopped. This paper had two vertical internal lines separated by a distance equal to the laser dot diameter and two external lines at a distance of 2 mm outside of the internal ones. A central line was the reference for marking the position of the laser dot. When the motion of the laser dot stopped, the piece of paper was placed in such a way that the light dots were inside the two internal lines. The external lines were used as a coarse reference that helped to center the laser dot. Thus, with the laser dot entirely placed between the external lines, the uncertainty associated with the position was below 2 mm. For a schematic visualization, see Fig. 1.

Taking into account that the expected increment of the oscillation amplitude was greater than 300 mm, this uncertainty implies an error of the measures smaller than 1%. The experimental setup is illustrated in Fig. 2.

The oscillations were registered on a flat plate placed at a distance of 5020 mm from the suspending wire of the pendulum. The endpoints of each oscillation were marked consecutively, according to Fig. 3.

In each test, the initial and final points of $n$ oscillations previous to the one in which the thruster was activated were registered and numbered consecutively. So, the $n$ oscillations were defined by $n + 1$ points. For each pair of points, $i$ and $i + 1$, the angular amplitude of the pendulum oscillation was calculated as follows (Fig. 4):

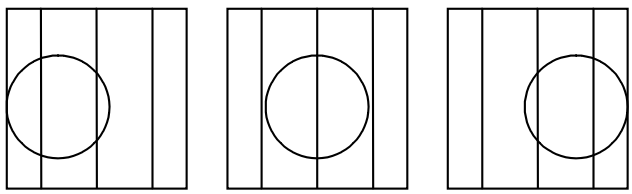

**Fig. 1 Recording of the laser dot position.**

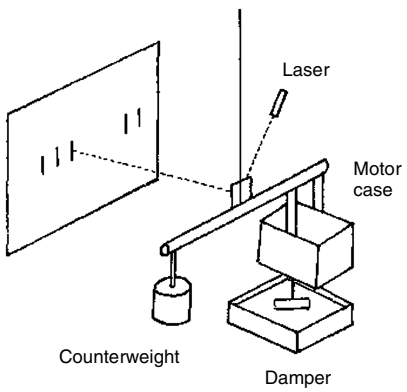


**Fig. 2 Experimental setup.**

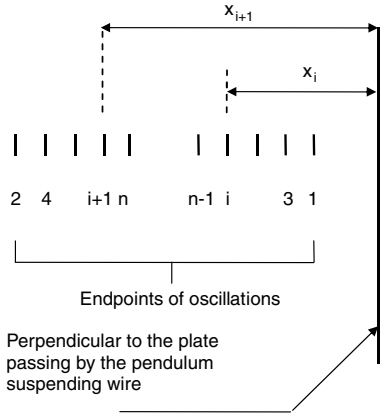


**Fig. 3 Recording of the endpoints of oscillations.**

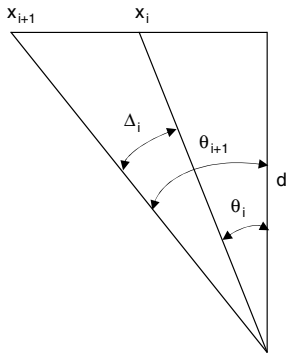


**Fig. 4 Linear and angular positions of the laser dots.**

$$\Delta_i = |\theta_{i+1} - \theta_i| \tag{3}$$

where

$$\theta_i = \tan^{-1}\left(\frac{x_i}{d}\right) \tag{4a}$$

$$\theta_{i+1} = \tan^{-1}\left(\frac{x_{i+1}}{d}\right) \tag{4b}$$

On the other hand, the angular amplitude of the oscillations can be estimated as

$$\Delta^* = \Delta_0 e^{pt} \tag{5}$$

where $\Delta_0$ is the initial angular amplitude or the amplitudes for $p = 0$. The amplitude of the first oscillation is

$$\Delta_i^* = \Delta_0 e^{pT/4} \tag{6}$$

the time $t$ corresponding to the middle point of the oscillation, which is $T/4$. For the second oscillation,

$$\Delta_2^* = \Delta_0 e^{p3T/4} \tag{7}$$

and so the time for the middle point of each oscillation is an odd multiple of $T/4$. For the oscillation number $i$,

$$\Delta_i^* = \Delta_0 e^{p(2i-1)T/4} \tag{8}$$

Taking logarithms

$$\ell_n \Delta_i^* = \ell_n \Delta_0 + p(2i-1)T/4 \tag{9}$$

The quadratic error $\varepsilon^2$ is the square of the difference between the measured value $\Delta$ and the estimated $\Delta^*$ of each oscillation:

$$\varepsilon_i^2 = [\ell_n \Delta_i - \ell_n \Delta_0 - p(2i-1)T/4]^2 = \ln^2\Delta_i + \ln^2\Delta_0 + p^2[(2i-1)T/4]^2 - 2\,\ell_n \Delta_0\,\ell_n \Delta_i - 2p\,\ell_n \Delta_i(2i-1)T/4 + 2p\,\ell_n \Delta_0(2i-1)T/4 \tag{10}$$

Calling

$$u_i = (2i-1)T/4 \tag{11a}$$

$$v_i = \ell_n \Delta_i \tag{11b}$$

the error can be put as

$$\varepsilon_i^2 = v_i^2 + \ln^2\Delta_0 + p^2u_i^2 - 2v_i\,\ell_n \Delta_0 - 2pu_iv_i + 2pu_i\,\ell_n \Delta_0 \tag{12}$$

For $n$ amplitudes, the total error is

$$\sum \varepsilon_i^2 = \sum v_i^2 + n\ln^2\Delta_0 + p^2\sum u_i^2 - 2\,\ell_n \Delta_0 \sum v_i - 2p\sum u_iv_i + 2p\,\ell_n \Delta_0 \tag{13}$$

The conditions that minimize the quadratic error are

$$\frac{\partial(\sum \varepsilon_i^2)}{\partial\,\ell_n \Delta_0} = 2n\,\ell_n \Delta_0 + 2p\sum u_i - 2\sum v_i = 0 \tag{14a}$$

$$\frac{\partial(\sum \varepsilon_i^2)}{\partial p} = 2p\sum u_i^2 + 2\,\ell_n \Delta_0 \sum u_i - 2\sum u_iv_i = 0 \tag{14b}$$

From the system of two equations,

$$n\,\ell_n \Delta_0 + p\sum u_i = \sum v_i \tag{15a}$$

$$\ell_n \Delta_0 \sum u_i + p\sum u_i^2 = \sum u_iv_i \tag{15b}$$

the values of $\Delta_0$ and $p$ are obtained:

$$\Delta_0 = \exp\left(\frac{\sum u_i^2 \sum v_i - \sum u_i \sum u_iv_i}{n\sum u_i^2 - (\sum u_i)^2}\right) \tag{16}$$

$$p = \frac{n\sum u_iv_i - \sum u_i \sum v_i}{n\sum u_i^2 - (\sum u_i)^2} \tag{17}$$

The correlation coefficient is given by

$$r = \frac{n\sum u_iv_i - \sum u_i \sum v_i}{\sqrt{[n\sum u_i^2 - (\sum u_i)^2]\,[n\sum v_i^2 - (\sum v_i)^2]}} \tag{18}$$

The closer to $\pm 1$ the value of $r$, the better the accuracy of the correlation. The angular middle point of each oscillation was calculated as

$$\bar{\theta}_i = (\theta_i + \theta_{i+1})/2 \tag{19}$$

where $\theta_i$ and $\theta_{i+1}$ are the angular positions given by Eqs. (4a) and (4b). The center of gravity of the middle points for $n$ oscillations is

$$\theta_m = \frac{\sum_{i=1}^n \bar{\theta}_i}{n} = \frac{1}{2n}\sum_{i=1}^n (\theta_{i+1} + \theta_i) \tag{20}$$

that, in a compact way, can be put as

$$\theta_m = \frac{\theta_1 + 2\sum_{i=2}^{n}\theta_i + \theta_{n+1}}{2\,n} \tag{21}$$

The positions of the calculated endpoints are given by

$$x_{c\,i} = d\tan(\theta_m + \theta_i^*) \tag{22}$$

where

$$\theta_i^* = \pm\Delta_0/2\exp[(i-1)pT/2] \tag{23}$$

The signs are + for $x_i > x_{i+1}$ and − for $x_i < x_{i+1}$.

The measured and calculated linear amplitudes of each oscillation were obtained, respectively, from

$$A_{m\,i} = |x_{i+1} - x_i| \tag{24a}$$

$$A_{c\,i} = |x_{c\,i+1} - x_{c\,i}| \tag{24b}$$

The mean quadratic error, taken as the mean quadratic difference between both amplitudes for $n$ oscillations, is given by

$$\sigma = \sqrt{\frac{\sum_{i=1}^{n}(A_{m\,i} - A_{c\,i})^2}{n}} \tag{25}$$

The general experimental procedure was as follows. For each test, with the measured positions of the laser light dots, the angular amplitudes of $n$ oscillations previous to those of the activation of the thrusters were calculated by means of Eq. (3), and the values of $\Delta_0$ and $p$ were calculated with Eqs. (16) and (17), respectively. The accuracy of the correlation was evaluated by means of Eq. (18). With the values of $\Delta_0$ and $p$, the estimated positions of the laser light dots on the plate were calculated with Eqs. (19–22), and the measured and calculated amplitudes were calculated with Eqs. (24a) and (24b). Then, the position of the laser light dot on the plate and the amplitude of the next oscillation (where the thruster was activated) were calculated, and these values were compared with the actual experimental ones. If some force acted, it would produce an increase in the amplitude of the experimental oscillation. Thus, since the calculated values were obtained assuming a free oscillation of the pendulum, if a significant increment of the experimental amplitude with respect to the calculated value had been observed, the acting force could be detected and evaluated. It was considered a significative difference between experimental and calculated amplitudes: greater than three times the mean quadratic error ($>3\sigma$).

To prevent overheating of the thrusters, the action time was limited to 20 s, much less than the period of the pendulum. Therefore, for maximizing the effect of the thrust (that is, the increment of the oscillation amplitude over the ones without thrust), it was necessary to set the time from the beginning of the oscillation at which the thrusters should be activated. For this, several simulations were carried out in which the amplitudes of oscillations with a constant force equal to the expected thrust were calculated by means of Eq. (2), with the force starting to be applied at different times from the beginning of the oscillation. The optimal result (that is, the maximum amplitude) was obtained when the force started to be applied at a quarter of the pendulum period minus a half of the action time of the thrusters: that is, with the action time centered at the middle of the oscillation.

Although the experiment was designed to evaluate a device that theoretically produced a thrust of 300 $\mu$N, a previous test with a 20 $\mu$N theoretical thrust motor was carried out. This motor had been tested before in a flexion pendulum setup, and the results were claimed as positive, although they were not conclusive in order to demonstrate the existence of a net propulsive force, since an oscillating force of null resultant would have produced a similar output signal. Therefore, it was decided first to test this motor, since the sensitivity of the torsion pendulum was good enough for detecting the expected force, and so a direct comparison with the flexion pendulum tests results could be done at once. Both the 20 $\mu$N and the 300 $\mu$N motors, run on the same theoretical fundamentals were (apart from the thrust and some minor details) essentially identical to those used in the tests mentioned in [1].

## III. Preliminary Test

The next step was the pendulum assembly. The length of the suspending wire was set at 2.35 m: the available height of the laboratory ceiling above the table supporting the experimental setup. To find the actual torsion stiffness of the suspending wire, the period of the calibration arm of known moment of inertia was measured. The calibration arm consisted of a 330-mm-diam and 16.25-kg-steel circular plate suspended perpendicularly to the wire in its center. The calculated value of the moment of inertia was 0.221 kg m$^2$; the period of oscillation, averaged over 10 semicycles, was found to be 81.5 s. Because the damping was very small, the final points in each semiamplitude of the oscillations were very close to each other, almost superposed, making it very difficult, if not impossible, to measure the position of each one. Therefore, only the positions of the endpoints of the first oscillation and those of the last one were measured, and they are shown in Table 2.

The amplitude of each oscillation and the times corresponding to their middle points are shown in Table 3.

The amplitudes can be estimated as

$$A_1 = A_0 e^{pt_1} \tag{26a}$$

$$A_2 = A_0 e^{pt_2} \tag{26b}$$

Taking logarithms

$$\ell_n A_1 = \ell_n A_0 + pt_1 \tag{27a}$$

$$\ell_n A_2 = \ell_n A_0 + pt_2 \tag{27b}$$

the damping factor is obtained by means of

$$p = \frac{\ell_n(A_2/A_1)}{t_2 - t_1} \tag{28}$$

With the data from Table 3, the damping factor results in $p \approx 0.00056$ s$^{-1}$. The torsion stiffness was obtained by means of

$$\frac{2\,\pi}{T} = \sqrt{\frac{k}{I} - p^2} \tag{29}$$

from where the value $k = 0.00131$ Nm/rad resulted, which is practically identical to that used in the preliminary estimations. It must be remarked that values of $p$ comprised between 0 and 0.0056 s$^{-1}$ (that is, 10 times greater than the calculated) do not substantially modify the calculated value of the torsion stiffness.

To experimentally verify the sensitivity of the torsion pendulum, the following test was carried out. A little pendulum, composed by a mass $m$ of 19 mg and a thread of mass $m_t \approx 10$ mg and 240 mm in

**Table 2 Calibration test**

| Point no. | $x$, mm |
|---|---|
| 1 | 139 |
| 2 | 169 |
| 9 | 142 |
| 10 | 167 |

**Table 3 Times and amplitudes**

| Oscillation | $t$, s | $A$, mm |
|---|---|---|
| 1–2 | 20.375 | 30 |
| 9–10 | 346.375 | 25 |

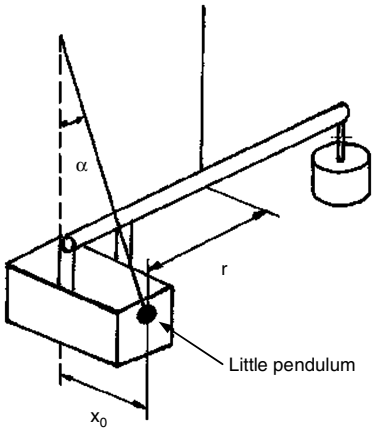


**Fig. 5 Simulation of thrust.**

length, was hung at a distance of nearly 210 mm from the suspension point of the torsion pendulum, with the little mass displaced from the vertical about 25 mm, pushing on the motor case and simulating a thrust, as schematically shown in Fig. 5.

The force produced by the little pendulum is caused by the masses $m$ and $m_t$, supposing that $m_t$ is concentrated at the middle of the thread length, and the angle $\alpha$ is very small and given by

$$F \cong mg\frac{x_0 - \Delta x}{l_t} + m_t g\frac{x_0 - \Delta x}{2l_t} = \left(m + \frac{m_t}{2}\right)g\frac{x_0 - \Delta x}{l_t} \quad (30)$$

where $x_0$ is the initial distance from the vertical line passing by the hanger point, and $\Delta x$ is the displacement of the mass due to the motion of the torsion pendulum. This displacement is proportional to the turn angle $\Delta\theta$ of the torsion pendulum, and it takes place until the moment of the acting force is balanced by the moment produced by the torsion of the suspending wire of the pendulum. Then, calling

$$m_e = m + m_t/2 \quad (31)$$

the equilibrium condition results in

$$M = \frac{m_e g r}{l_t}(x_0 - r\Delta\theta_f) = k\Delta\theta_f \quad (32)$$

The final torsion angle is obtained from

$$\Delta\theta_f = \frac{x_0}{r + kl_t/m_e g r} \quad (33)$$

The corresponding linear displacement of the laser dot on the wall is

$$\delta \cong 2d\Delta\theta_f = \frac{2dx_0}{r + kl_t/m_e g r} \quad (34)$$

So, for $d = 5020$ mm, $x_0 = 25$ mm, $r = 210$ mm, $k =$ 0.00131 Nm/rad, $m = 19$ mg, $m_t = 10$ mg, and $l = 240$ mm, a mean force of about 25 $\mu$N results, and a displacement of $\delta \approx$ 38 mm is obtained.

On the other hand, three experimental tests were carried out. In the first test, the torsion pendulum oscillated freely without force applied on it. In the second test, the mass of the little pendulum pushed against the motor case while the torsion pendulum oscillated and, in the third test, the little pendulum was separated from the motor case, which continued oscillating. In all the tests, the endpoints of the oscillations were recorded, and the results are shown in Table 4.

For each test, the middle point of the set of oscillations was calculated by means of an equation similar to Eq. (21):

$$x_m = \frac{x_1 + 2\sum_{i=2}^{n-1} x_i + x_n}{2\,(n-1)} \quad (35)$$

and the standard deviation was calculated by means of

**Table 4 Positions of the endpoints**

| | $x$, mm | | |
|---|---|---|---|
| Point no. | Without force | With force | Without force |
| 1 | 478 | 621 | 633 |
| 2 | 676 | 483 | 530 |
| 3 | 495 | 601 | 623 |
| 4 | 661 | 495 | 540 |
| 5 | 507 | 587 | 615 |
| 6 | 647 | 507 | 545 |
| 7 | 520 | 577 | 608 |
| 8 | 635 | 516 | 550 |
| $x_m$ | 580 | 545 | 579 |
| Sd | 3.5 | 3.7 | 2.0 |

$$\text{Sd} = \sqrt{\frac{\sum_{i=1}^{n-1}[(x_i + x_{i+1})/2 - x_m]^2}{n-1}} \quad (36)$$

These values are shown in the two last rows of Table 4. It can be seen that the first value and the third of the middle points with no acting force are practically identical, while the second value is shifted about 35 mm from the other two. This value is very close to that previously obtained by means of Eq. (34). The small difference between both results is due to experimental errors, since it is of the same magnitude as the standard deviations shown in Fig. 4. In this way, the capability of the torsion pendulum to detect a force much smaller than the one expected was experimentally verified.

## IV. Experimental Results

As explained previously, two sets of tests were carried out: the first set with a motor of about 20 $\mu$N of theoretical thrust and the second set with a motor of about 300 $\mu$N. These thrusts were experimentally confirmed by another working team using a flexion pendulum setup. Apart from the thrust and some little details, both motors were essentially identical.

### A. Tests with 20 $\mu$N Thrust Motor

A total of six tests were carried out. Since the results were practically identical, only three of them are shown and analyzed here. The distances of the endpoints of the oscillations, measured from the plane perpendicular to the recording plate passing by the suspension wire of the pendulum, are shown in Table 5. The pendulum period was 138 s, and the time interval between two consecutive measures was one half of the period: that is, 69 s.

Points 1 to 10 correspond to pendulum-free oscillation. Thruster activation proceeded from points 10 to 11. For a quick visual inspection, as a coarse way to detect any significant anomaly, the data from the Table are graphically displayed in Figs. 6–8.

The actual ($x_i$) and calculated ($x_{c\,i}$) positions of the endpoints, as well as the measured ($A_m$) and calculated ($A_c$) amplitudes, are shown in Tables 6–8. For Table 6, the initial angular amplitude was 0.008785 rad, the damping factor was $-0.001061$ s$^{-1}$, the

**Table 5 Positions of endpoints**

| | $x$, mm | | |
|---|---|---|---|
| Point no. | Test 1 | Test 2 | Test 3 |
| 1 | 916 | 433 | 169 |
| 2 | 829 | 382 | 278 |
| 3 | 911 | 430 | 177 |
| 4 | 836 | 385 | 270 |
| 5 | 907 | 425 | 186 |
| 6 | 842 | 389 | 264 |
| 7 | 904 | 423 | 191 |
| 8 | 849 | 391 | 258 |
| 9 | 903 | 421 | 197 |
| 10 | 855 | 393 | 254 |
| 11 | 900 | 419 | 202 |

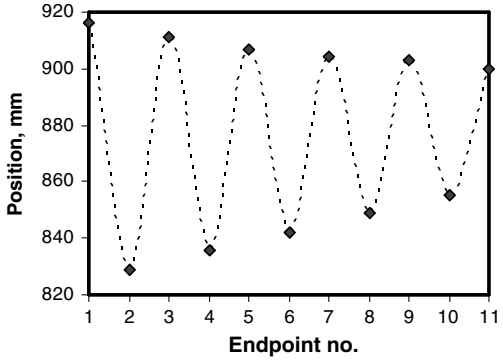


**Fig. 6 Test 1 positions of endpoints.**

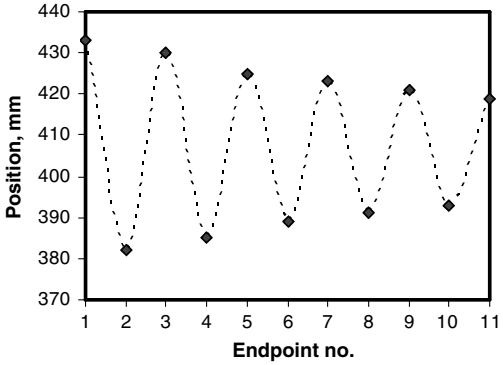


**Fig. 7 Test 2 positions of endpoints.**

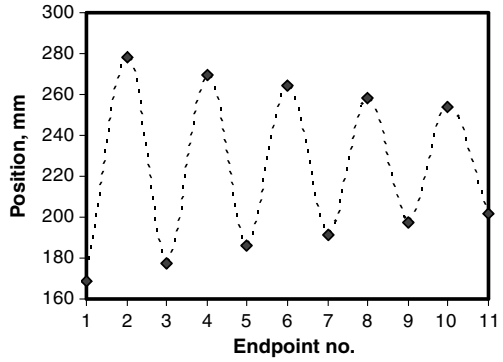


**Fig. 8 Test 3 positions of endpoints.**

correlation coefficient was −0.9961, and the mean quadratic error was 0.927 mm. For Table 7, the initial angular amplitude was 0.005254 rad, the damping factor was −0.001124 $s^{-1}$, the correlation coefficient was−0.9950, and the mean quadratic error was 0.750 mm. For Table 8, the initial angular amplitude was 0.01128 rad, the damping factor was −0.001184 $s^{-1}$, the correlation coefficient was −0.9993, and the mean quadratic error was 0.582 mm. As can be seen from the three tables, the final (extrapolated) calculated amplitudes without thrust are (within the experimental errors) equal to the correspondent experimental amplitudes when the device was activated. Therefore, it is concluded that no net force acted during this oscillation, apart from the damping.

**Table 6 Test 1: Positions and amplitudes**

| $i$ | $x_i$ | $x_{i+1}$ | $x_{c\,i}$ | $x_{c\,i+1}$ | $A_m$ | $A_c$ |
|---|---|---|---|---|---|---|
| 1 | 916 | 829 | 920 | 832 | 87 | 88 |
| 2 | 829 | 911 | 832 | 913 | 82 | 81 |
| 3 | 911 | 836 | 913 | 838 | 75 | 76 |
| 4 | 836 | 907 | 838 | 908 | 71 | 70 |
| 5 | 907 | 842 | 908 | 843 | 65 | 65 |
| 6 | 842 | 904 | 843 | 903 | 62 | 61 |
| 7 | 904 | 849 | 903 | 847 | 55 | 57 |
| 8 | 849 | 903 | 847 | 899 | 54 | 53 |
| 9 | 903 | 855 | 899 | 851 | 48 | 49 |
| 10 | 855 | 900 | 851 | 896 | 45 | 45 |

**Table 7 Test 2: Positions and amplitudes**

| $i$ | $x_i$ | $x_{i+1}$ | $x_{c\,i}$ | $x_{c\,i+1}$ | $A_m$ | $A_c$ |
|---|---|---|---|---|---|---|
| 1 | 433 | 382 | 433 | 382 | 51 | 51 |
| 2 | 382 | 430 | 382 | 429 | 48 | 47 |
| 3 | 430 | 385 | 429 | 386 | 45 | 44 |
| 4 | 385 | 425 | 386 | 426 | 40 | 41 |
| 5 | 425 | 389 | 426 | 389 | 36 | 37 |
| 6 | 389 | 423 | 389 | 423 | 34 | 35 |
| 7 | 423 | 391 | 423 | 391 | 32 | 32 |
| 8 | 391 | 421 | 391 | 421 | 30 | 30 |
| 9 | 421 | 393 | 421 | 393 | 28 | 28 |
| 10 | 393 | 419 | 393 | 419 | 26 | 26 |

**Table 8 Test 3: Positions and amplitudes**

| $i$ | $x_i$ | $x_{i+1}$ | $x_{c\,i}$ | $x_{c\,i+1}$ | $A_m$ | $A_c$ |
|---|---|---|---|---|---|---|
| 1 | 169 | 278 | 169 | 278 | 109 | 109 |
| 2 | 278 | 177 | 278 | 178 | 101 | 100 |
| 3 | 177 | 270 | 178 | 270 | 93 | 93 |
| 4 | 270 | 186 | 270 | 185 | 84 | 85 |
| 5 | 186 | 264 | 185 | 264 | 78 | 79 |
| 6 | 264 | 191 | 264 | 191 | 73 | 73 |
| 7 | 191 | 258 | 191 | 258 | 67 | 67 |
| 8 | 258 | 197 | 258 | 196 | 61 | 62 |
| 9 | 197 | 254 | 196 | 253 | 57 | 57 |
| 10 | 254 | 202 | 253 | 201 | 52 | 52 |

### B. 300 $\mu$N Thrust Motor

Two tests were carried out. The positions of the endpoints of the oscillations are shown in Table 9. The pendulum period was 168 s, and the time interval between two consecutive measures was one half of the period: that is, 84 s. The data from the table are graphically displayed in Figs. 9 and 10.

The actual ($x_i$) and calculated ($x_{c\,i}$) positions of the endpoints, as well as the measured ($A_m$) and calculated ($A_c$) amplitudes are shown in Tables 10 and 11. In Table 10, the initial angular amplitude was 0.01142 rad, the damping factor was −0.000975 $s^{-1}$, the correlation coefficient was −0.9996, and the mean quadratic error was 0.817 mm. For Table 11, the initial angular amplitude was 0.009116 rad, the damping factor was −0.001053 $s^{-1}$, the correlation coefficient was −0.9714, and the mean quadratic error was 2.861 mm.

**Table 9 Positions of endpoints**

| | $x$, mm | |
|---|---|---|
| Point no. | Test 1 | Test 2 |
| 1 | 149 | 251 |
| 2 | 259 | 165 |
| 3 | 157 | 244 |
| 4 | 251 | 171 |
| 5 | 165 | 238 |
| 6 | 244 | 175 |
| 7 | 171 | 232 |
| 8 | 238 | 177 |
| 9 | 175 | 228 |
| 10 | 232 | 190 |
| 11 | 177 | 225 |

**Table 10 Test 1: Positions and amplitudes**

| $I$ | $x_i$ | $x_{i+1}$ | $x_{c\,i}$ | $x_{c\,i+1}$ | $A_m$ | $A_c$ |
|---|---|---|---|---|---|---|
| 1 | 149 | 259 | 148 | 259 | 110 | 111 |
| 2 | 259 | 157 | 259 | 157 | 102 | 102 |
| 3 | 157 | 251 | 157 | 251 | 94 | 94 |
| 4 | 251 | 165 | 251 | 164 | 86 | 87 |
| 5 | 165 | 244 | 164 | 244 | 79 | 80 |
| 6 | 244 | 171 | 244 | 170 | 73 | 74 |
| 7 | 171 | 238 | 170 | 238 | 67 | 68 |
| 8 | 238 | 175 | 238 | 176 | 63 | 62 |
| 9 | 175 | 232 | 176 | 233 | 57 | 57 |
| 10 | 232 | 177 | 233 | 180 | 55 | 53 |

**Table 11 Test 2: Positions and amplitudes**

| $i$ | $x_i$ | $x_{i+1}$ | $x_{c\,i}$ | $x_{c\,i+1}$ | $A_m$ | $A_c$ |
|---|---|---|---|---|---|---|
| 1 | 251 | 165 | 251 | 164 | 86 | 88 |
| 2 | 165 | 244 | 164 | 244 | 79 | 80 |
| 3 | 244 | 171 | 244 | 170 | 73 | 74 |
| 4 | 171 | 238 | 170 | 238 | 67 | 67 |
| 5 | 238 | 175 | 238 | 176 | 63 | 52 |
| 6 | 175 | 232 | 176 | 233 | 57 | 56 |
| 7 | 232 | 177 | 233 | 181 | 55 | 52 |
| 8 | 177 | 228 | 181 | 228 | 51 | 47 |
| 9 | 228 | 190 | 228 | 185 | 38 | 43 |
| 10 | 190 | 225 | 185 | 225 | 35 | 40 |

Some differences exist between the experimental amplitudes with the thruster switched on and the ones calculated without thrust, but since they are smaller than $3\sigma$, they are considered nonsignificant. On the other hand, in the first test, the experimental amplitude was greater than the calculated one, but in the second test, the inverse occurred. This means that these differences are not systematic but random due to experimental errors; therefore, they cannot be attributed to an actual propulsive effect.

## V. Analysis of Results

In none of the tests, was a significative increment of the amplitudes with respect to the expected values without thrust obtained. The anomalous behavior observed in Figs. 9 and 10 was probably caused by a coupling between angular and linear oscillations, since the setup can oscillate as an ordinary pendulum. Thus, the angular oscillations could have been modulated by the linear oscillations. To estimate the amplitudes with thrust and compare with experimental results, these were calculated for each test by means of Eq. (2) in the following way.

The initial angular amplitude of the oscillation in which the device was activated can be estimated by means of an equation similar to Eq. (7):

$$\Delta_0 = \text{abs}[\tan^{-1}(x/d) - \tan^{-1}(x^*/d)]\exp(pT/4)/2 \tag{37}$$

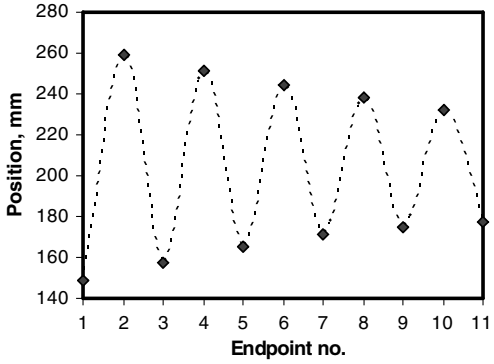


**Fig. 9 Test 1 positions of endpoints.**

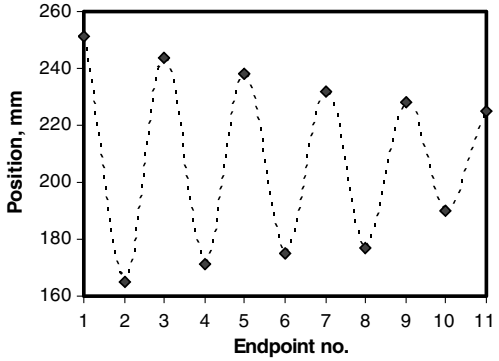


**Fig. 10 Test 2 positions of endpoints.**

where $x^*$ is the position of the point where the oscillation with the device activation began, and $x$ is the position of the immediately previous endpoint. The factor of two, dividing the equation, is because the mirror duplicates the angle of the laser beam with respect to the torsion angle of the pendulum. The initial angular position of the oscillation where the thruster was activated is

$$\theta_0 = \tan^{-1}(x^*/d) \tag{38}$$

With the initial semiamplitude and the damping factor, two calculations were carried out: one without thrust and the other with thrust. In both cases, the angular amplitude of each one of the oscillations were obtained, and the final angular position $\theta_c$ and final linear position $x_c$ were calculated from

$$\theta_c = \theta_0 + 2\Delta \tag{39}$$

$$x_c = d\tan\theta_c \tag{40}$$

The linear amplitude of the oscillation is

$$A_c = |x_c - x^*| \tag{41}$$

So, two values of calculated linear amplitudes were obtained for each test: one without thrust and the other with the nominal expected thrust. These values are shown in Tables 12 and 13.

As can be seen, in both cases, the experimental amplitudes are very close or identical to the ones calculated without thrust, and they are much smaller than the expected amplitudes with thrust. The differences between experimental and calculated with thrust amplitudes, already big in the case of the 20 $\mu$N motor, are considerable for the 300 $\mu$N motor.

**Table 12 20 $\mu$N thrust motor**

| Test no. | Amplitudes, mm | | |
|---|---|---|---|
| | Calculated with thrust | Calculated without thrust | Measured |
| 1 | 73 | 45 | 45 |
| 2 | 53 | 26 | 26 |
| 3 | 80 | 53 | 53 |

**Table 13 300 $\mu$N thrust motor**

| Test no. | Amplitudes, mm | | |
|---|---|---|---|
| | Calculated with thrust | Calculated without thrust | Measured |
| 1 | 390 | 53 | 55 |
| 2 | 374 | 35 | 35 |

To end this work appropriately, a brief reference to the results obtained with the flexion pendulum should be done. The oscillating force detected with this setup can be owed to two possible causes: by a genuine effect related in any way with the theory despite the absence of a net propulsive force or by the action of spurious effects. Some of them were mentioned in [1] but disregarded by estimating their contribution negligible. Nevertheless, one of them should be analyzed more carefully, which is the electromagnetic interaction. In fact, flexible wires can oscillate due to the electromagnetic forces caused by the interaction between the electric current they conduct and the magnetic fields produced by other wires and devices: for example, the toroidal coil. A very simple estimation can be carried out, considering a copper wire of a 0.5 mm diameter that is 100 mm long for which the center of mass oscillates at approximately 25 Hz (a typical frequency used in the tests), with a semiamplitude $A$ of 10 $\mu$m. The mass of the wire is of about $1.5 \times 10 - 4$ kg, and the force acting on it can be estimated as

$$F \approx m\omega^2 A = m(2\pi f)^2 A \tag{42}$$

Thus, an oscillating force of approximately 35 $\mu$N results. If several wires are considered instead of one, a similar force could be obtained with a much smaller amplitude of oscillation or greater forces with the same amplitude. Therefore, more tests, very careful, should be carried out to conclusively determine the real cause that produces the observed effect.

## VI. Conclusions

The experimental results with the torsion pendulum show conclusively that no propulsive forces of the magnitude expected, neither much smaller than these, were produced by the devices. These results are in contradiction with those obtained before with the flexion pendulum setup. Most likely, the oscillating force detected with the flexion pendulum was caused by some spurious effect. Otherwise, if a genuine force (net or oscillating) was produced by the device, it would be a perpetual motion machine, at least in a conceptual sense.

## References

[1] Brito, H. H., and Elaskar, S. A., "Direct Experimental Evidence of Electromagnetic Inertia Manipulation Thrusting," *Journal of Propulsion and Power*, Vol. 23, No. 2, 2007, pp. 487–494. doi:10.2514/1.18897

[2] Marini, R., "Comment on Direct Experimental Evidence of Electromagnetic Inertia Manipulation Thrusting," *Journal of Propulsion and Power*, Vol. 25, No. 2, 2009, pp. 543–544. doi:10.2514/1.33196

G. Spanjers
*Associate Editor*